

Performance evaluation of 2-channel endorectal coil geometries for imaging the prostate at 7T

M. Arcan Erturk¹, Gregor Adriany¹, and Gregory J Metzger¹

¹Center for Magnetic Resonance Research, University of Minnesota, Minneapolis, Minnesota, United States

Audience. Researchers interested in prostate imaging and/or coil development.

Purpose. Compared to the external surface array (ESA), endorectal coils (ERCs) can improve the signal-to-noise ratio (SNR) inside the prostate by more than 4-fold at 7T^{1,2}. Solid ERCs (sERCs) that can be inserted inside a rigid, sterilizable external housing is a viable alternative to disposable balloon-type ERCs. In this study, we compare three different 2-channel sERC geometries for imaging the prostate at 7 T in terms of their transmit (B_1^+) and receive (SNR) performance inside a torso-sized phantom.

Methods. Two Loop Design (ERC-2OL): The two loop ERC (ERC-2OL) was built by placing two rectangular loops on a 2.2cm diameter 7.2cm long cylindrical core (Hologic, Toronto, ON). The short axis of each loop was 1.9cm and length was 7.1cm. The loops were overlapped by 0.3cm.

Stripline and Loop Designs: Two others ERCs were built by combining a resonant stripline element with a large or small rectangular loop element. They were built on 1.9cm diameter 5.5cm long cylindrical rods. The ground plane of the stripline elements were placed at the center axis of the rods. Rectangular loops were centered around the copper conductor on the cylindrical rod surface. Long axis lengths of the loops were 6.7cm. Short axis lengths of the rectangular loops varied between 2.2cm for ERC-SLL and 1.4cm for ERC-SSL. Coils were tuned for ¹H at 7T. Geometries of three coil designs (ERC-2OL, ERC-SLL, ERC-SSL) are shown in Fig. 1.

Performance Evaluation: MRI experiments were conducted on a Magnetom 7T scanner (Siemens Healthcare, Erlangen, Germany) inside a 18L torso-sized phantom filled with a loading solution¹. Coils were inserted in a 2.55cm diameter cylindrical housing (Hologic Inc.), and placed inside the phantom. SNR data were acquired using a gradient echo sequence with TR/TE=10s/3.8ms, FA=90°, voxel-size=1.5x1.5x3mm³, followed by a noise scan. Normalized SNR maps were calculated according to the methods of Edelstein et al.³. B_1^+ maps were calculated using the flip-angle map acquired via the actual flip angle technique⁴. SNR and B_1^+ performance of a 16-channel transceive stripline array (ESA)⁵ were also computed using the same methods.

Results and Discussion. Coupling between the channels (S21) of the stripline loop combinations were lower than -15dB, and -10.4dB for the two-loop design (Table I). ERC-SSL had the best SNR and transmit performance inside an ROI (dimensions: 3.75x2.4x2.7cm³) representing the prostate (Fig. 2, 3, Table I). Despite having better directionality, the small width of the ERC-SSL loop resulted in a reduced performance at depths >4cm compared to ERC-2OL. Simulations of the ERC-SSL are required to qualify the performance gains against specific absorption rate (SAR) estimates. Compared to the ESA, ERCs provided ~5-fold SNR and B_1^+ efficiency improvement.

Conclusion. A reusable, 2-channel ERC improves the performance of prostate MRI at 7T by ~5-fold compared to an ESA. A stripline-small loop configuration (ERC-SSL) yielded the best performance in phantom studies compared to the previously presented two loop design⁶.

References. [1] Metzger (2010) MRM 64:1625-1639. [2] de Castro (2012) MRM 68:311-318. [3] Edelstein (1986) MRM 3:604-618. [4] Yarnykh (2007) MRM 57:192-200. [5] Metzger (2012) MRM 67:954-964. [6] Metzger (2014) ISMRM p626.

Acknowledgements. Funding support by: NCI R01 CA155268, WM Keck Foundation, S10 RR026783, NIBIB P41 EB015894. We thank Matt Waks (Virtumed LLC, Minneapolis, MN) for help with the ERCs.

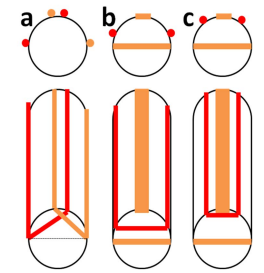


Fig. 1. Schematic drawings of (a) ERC-2OL, (b) ERC-SLL, (c) ERC-SSL. Top row shows the axial cross-section and the bottom row depicts the view from top. Orange and red colors represent the channels of the coil.

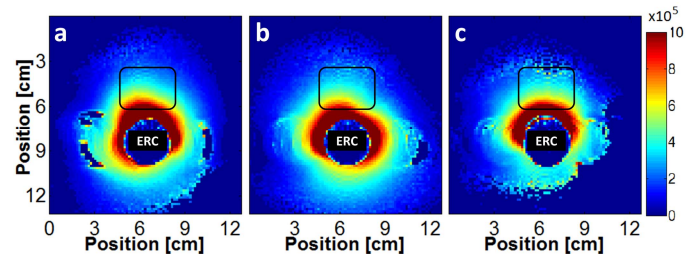


Fig. 2. Sum of magnitude SNR in Hz^{0.5}/ml of (a) ERC-2OL, (b) ERC-SLL, and (c) ERC-SSL are shown. Black annotated boxes show the ROIs used for computation of the numbers in Table I.

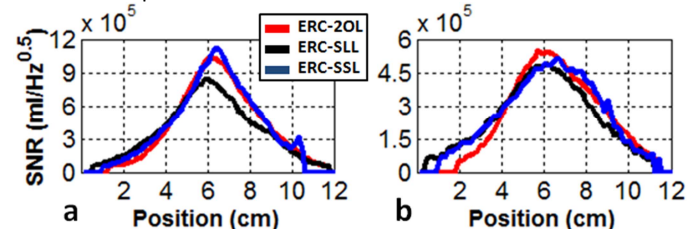


Fig. 3. SNR profiles of ERC-2OL, ERC-SLL, and ERC-SSL (red, black, and blue, respectively) along L-R dimension (a) 1cm, and (b) 2cm anterior to the coils

| | ERC-2OL | ERC-SLL | ERC-SSL | ESA |
|--|-----------|-----------|-----------|-----------|
| S21 (dB) | -10.4 | -17.7 | -15.3 | n/a |
| SNR (Hz ^{0.5} /ml) x10 ⁵ | 5.33±2.56 | 4.56±1.84 | 5.41±2.98 | 0.96±0.08 |
| Difference | 0 | -14.4% | +1.5% | -82.0% |
| B ₁ ⁺ (μT/W ^{0.5}) | 1.08±0.32 | 0.99±0.41 | 1.16±0.71 | 0.18±0.02 |
| Difference | 0 | -8.3% | +8.2% | -83.7% |

Table I. Mean and standard deviation of the SNR and transmit efficiency computed inside the black ROI shown in Fig. 2 are listed for ERC-2OL, ERC-SLL, ERC-SSL, and ESA.